Structure of Sn/Ge(111) from low-energy electron-diffraction and photoemission studies

S. B. DiCenzo, P. A. Bennett,* D. Tribula,† P. Thiry,‡ G. K. Wertheim, and J. E. Rowe§
AT&T Bell Laboratories, Murray Hill, New Jersey 07974
(Received 3 August 1984)

High-resolution photoemission measurements ($\Delta E \approx 200$—250 meV) have been made on Ge $3d$ and Sn $4d$ core levels using synchrotron radiation from the National Synchrotron Light Source at Brookhaven National Laboratory. Systematic analysis using nonlinear least-squares fits has shown evidence for three different Ge components and two different Sn components. The selective modification of one Ge component as a function of Sn coverage leads to some quantitative restrictions on structural models for the Sn-induced 7×7 and 5×5 reconstructed superlattices. In particular, simple adatom models, vacancy models, and buckling models are not fully consistent with our results. A multilayer adatom model, such as the "tripedal" model of Aono *et al.* [Phys. Rev. Lett. 51, 801 (1983)] is found to be the most plausible one to interpret our results.

I. INTRODUCTION

Current studies of the geometric and electronic structure of the Ge(111) surface, both clean[1–3] and with metal[4] overlayers, seek to delineate the surface structure on an atomic scale, as well as the mechanism[5] which reduces the free energy leading to a reconstructed superlattice, e.g., 2×8, 7×7, or 5×5. The formation of the Schottky barrier at the metal-semiconductor interface also presents unsolved problems. Also of interest are changes in the band bending as the metallic overlayer is built up, and the identification of specific surface or interface states responsible for the pinning of the Fermi level.

Recently, the use of synchrotron radiation has allowed high-resolution ($\Delta E \approx 0.2$ eV) core-level photoemission to be performed over a range of kinetic energies from 5 to 100 eV.[1,6,7] Because the electron-escape length is energy dependent, control of the photon energy allows one to vary the surface-to-bulk sensitivity by nearly a factor of 10. Previous studies on semiconductors[6,7] have revealed surface core-level shifts in opposite directions for group-III and group-V elements of (110) faces of III-V compounds. In addition, core-electron binding energies at the Si(111) and Ge(111) surfaces depend upon the long-range periodicity, e.g., 1×1, 7×7, or 2×1. Thus, we expect that coverage-dependent surface signals and varying periodicity should be correlated for the present case of Sn/Ge(111) surfaces.

The choice of tin as an overlayer is favorable in that the solid solubility of Sn in Ge and of Ge in Sn are both $\sim1\%$, sufficiently small to preclude alloy formation.[8] Mössbauer-spectroscopy studies yield a maximum solid solubility of 5×10^{20} cm^{-3}, in good agreement with metallurgical studies. The small solubility of Sn in Ge is probably a result of the large difference in lattice constants between Ge, $a=5.646$ Å, and α-Sn, $a=6.489$ Å. Another practical advantage of this system for a photoemission study is that the Sn $4d$ and Ge $3d$ core levels are narrow, and their binding energies of 29 and 24 eV, respectively, are readily accessible with our high-resolution monochromator.

Tin may be expected to develop a variety of bonding configurations at the interface with germanium, since from the Pauling electronegativity difference of $\Delta\chi \approx 0.2$, one expects the Ge—Sn bonding to be moderately covalent. One might expect that Sn might substitute for Ge in the lattice or grow epitaxially on the Ge surface because Sn and Ge have similar bonding configurations in corresponding materials (e.g., Ge and α-Sn, or Mg_2Ge and Mg_2Sn).

A previous study[9] of Sn/Ge(111) has shown that a variety of ordered structures (viz., 2×2, 7×7, and 5×5) occur. Of particular interest is the occurrence of a 7×7 structure, since this could provide insight into the 7×7 reconstruction of the clean Si(111) surface.

II. EXPERIMENTAL DETAILS

A. Sample preparation

The (5×15)-mm^2 germanium samples were cut from n-type crystals with resistivities of 1—5 Ω cm. They were cleaned by sputtering with 500-eV argon ions for 30 min, and then annealing at 650 °C for 10 min. Cleanliness was verified by Auger scans in which the carbon and oxygen *KLL* Auger intensities were less than 1% of the germanium *LMM* Auger intensity, at 1150 eV. This cleaning procedure produced a sharp $c(2\times8)$ low-energy electron-diffraction (LEED) pattern, as well as valence-band features and core-level spectra characteristic of the clean, annealed surface.

The tin evaporator consisted of a collimator and shutter mechanism and a tungsten-ribbon oven constructed to encapsulate 0.4—1.0 g of tin. For each deposition the oven was preheated to ~1000 °C for 1 min before the shutter was opened. The pressure increase in the main chamber was $\sim1\times10^{-10}$ Torr. Typical exposure rates were ~0.1 monolayer per min [1 monolayer (ML) = 7.3×10^{14} atoms/cm^2].

After each deposition the sample was annealed for 1 min at 550 °C before the Auger or photoemission spec-

trum was recorded. At one coverage the spectrum was also recorded before annealing. The relative coverage for each deposition was determined by assuming that the sticking coefficient was independent of coverage, so that the total time of exposure to the tin source is used as a measure of relative coverage. The coverage scale was calibrated by ion-backscattering analysis[10] on several samples after removal from the vacuum system. The deposition rate was thereby determined to be 5.4×10^{13} cm^{-2}min^{-1} or 0.075 ML/min. The coverages are believed to be accurate to within $\sim10\%$. At submonolayer coverages, annealing changed the surface coverage by less than 5%, but at higher coverages there was a substantial decrease in Sn intensity, probably due to evaporation of Sn.

B. LEED and Auger measurements

Low-energy electron diffraction and Auger-electron spectroscopy (AES) were performed in an ion-pumped ultrahigh-vacuum (UHV) chamber at AT&T Bell Laboratories that has been previously described.[11] Some angle-integrated photoemission measurements of valence-band spectra were performed at resonance lamp energies of 11.7, 16.8, and 21.2 eV. This allowed us accurately to reproduce Sn-coverages at the Brookhaven Synchrotron Laboratory in a different UHV chamber which had AES and photoemission but not LEED capability. Most of the details of the two-dimensional (2D) phase diagram determined by Ichikawa and Ino[12] were verified as further discussed in Sec. III A.

C. Photoemission measurements

The photoemission experiments were performed on the AT&T Bell Laboratories beamline U4B at the National Synchrotron Light Source using a 6-m high-resolution toroidal-grating monochromator. A double-pass cylindrical mirror analyzer (CMA) was used both for Auger analysis and photoemission measurements. The incident-photon-beam direction was 45° to the sample normal, and the plane of polarization was parallel to the plane of incidence, i.e., p polarization. The CMA axis was also at 45° to the sample, but perpendicular to the photon beam. An energy resolution of 200–250 meV was estimated from the Fermi edge in a spectrum taken on a silver foil. All photoemission spectra were taken in the angle-integrating mode.

A photon energy of 68 eV was used for most of the spectra since it matches the "best-focus" condition for the monochromator. It also provides good surface sensitivity since the kinetic energy ($E\approx34$ eV for Ge $3d$ photoelectrons) lies near the minimum of the escape-depth curve ($\lambda\approx5$–6 Å for Ge). For the clean Ge surface, a series of core-level spectra was also taken with lower photon energies. The lower kinetic energy results in a longer mean free path (we estimate $\lambda\approx15$ Å at $h\nu=39$ eV or $E\approx5$ eV) for the photoelectrons, allowing us to emphasize the bulk contribution to the spectrum.

III. EXPERIMENTAL RESULTS AND ANALYSIS

A. LEED observations

The LEED patterns for the clean Ge(111) surface showed strong $\frac{1}{2}$-order spots and only those $\frac{1}{8}$-order spots nearest to the $\frac{1}{2}$-order ones, in agreement with earlier work. Upon deposition of ~0.1–0.2 ML of tin, the LEED pattern remained similar to that of the high-temperature phase of clean Ge(111), although blurred and reduced in intensity; this region is labeled diffuse 2×2. With further tin deposition, to coverages of 0.2–0.3 ML, the previously reported diffuse $(\sqrt{3}\times\sqrt{3})R30°$ pattern was *not* observed. However, a brief anneal at 250 °C produced a clear 7×7 pattern, which could be obtained at coverages between 0.25 and 0.5 ML.[9] As is the case for the Si(111)7×7 surface, spots near the $\frac{1}{2}$-order position were more intense. During these heating experiments, the $(\sqrt{3}\times\sqrt{3})R30°$ structure was not observed, although it may have occurred briefly during the annealing at temperatures at which we did not make LEED observations. The $\frac{1}{7}$-order reflections disappeared quickly in a reversible phase transition near 450 °C. For higher coverages (0.4–0.6 ML), a mixed pattern with both 5×5 and 7×7 features also appeared and is labeled "pseudo-12×12." Overall, our measurements confirm most of the general features of the phase diagram of Ichikawa;[9] our LEED results are summarized in the phase diagram shown in Fig. 1.

B. Data analysis of core-level line shapes

Our analyses were performed on data as taken, without prior background subtraction. A nonlinear least-squares program due to Marquardt[13] was used. The core-level peaks were fitted with model functions that incorporate

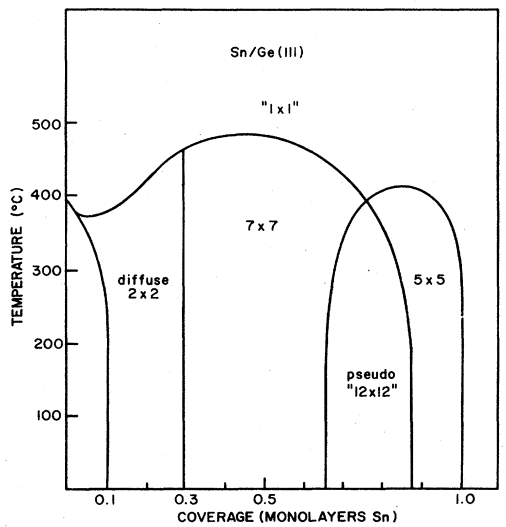

FIG. 1. Phase diagram of the Sn/Ge(111) surface. The low-coverage, low-temperature phase has a diffuse 2×8 periodicity.

the essential physics of the photoemission process. Each line is represented by a Lorentzian whose width corresponds to the lifetime of the hole state produced by photoemission. This line is convolved with a Gaussian whose width is the quadratic sum of the instrumental resolution and the width due to other processes, such as inhomogeneous broadening and phonon excitation. The background of secondary electrons is represented by a quadratic function whose three parameters are also adjusted during the least-squares optimization. For metals (e.g., Sn layers), the metallic screening response is introduced into the model function by replacing the Lorentzian with the line shape of Doniach and Šunjić.[14] This line shape is a convolution of the lifetime Lorentzian with the power-law line shape, which represents the effect of the conduction-electron screening response.

In general, the two lines of a spin-orbit doublet are specified by three parameters: the splitting, the intensity ratio, and the ratio of the two lifetime widths. However, the closely spaced lines in the Ge $3d$ doublets were assumed to have the same width, so that each doublet is specified by only two additional parameters, the relative energy and intensity. We found branching ratios of 0.64—0.68 (close to the statistical value of 0.667) and a spin-orbit splitting of 0.585 eV, consistent with earlier observations.[7]

The fitting program minimizes the sum of the squares of the residuals, the differences between the data points and the fitted curve. Because the detection of the photoelectrons is a Poisson-distributed process, the standard deviation of each channel in the spectrum is equal to the square root of the number of counts in that channel. Hence, as the fit is optimized, the ratio of the sum of the squares of the deviations to the sum of the counts in all the channels will approach unity. This ratio provides an objective test of the overall quality of the fit. A better and more detailed test of the quality of the fit is found in the spectrum of the residuals, which for an ideal fit consists entirely of the uncorrelated statistical fluctuations of the individual data points.

C. Ge $3d$ spectra for the clean Ge(111)2×8 surface

For analyzing the Ge core-level spectra we chose a model function containing three spin-orbit doublets. The motivation for our choice is illustrated in Fig. 2. Both halves of the figure show the same spectrum, obtained for a clean Ge(111) surface with a photon energy of 68 eV. The solid curve through the data points in Fig. 2(a) is a fit using a model consisting of two spin-orbit doublets constrained to have the same line shapes and spin-orbit parameters. Although superficially the fit appears to be satisfactory, an examination of the residuals reveals problems. Not only are the residuals themselves much greater than expected on the basis of the number of counts in each channel, but also they are oscillatory, with a period roughly equal to the width of the lines fitted to the data. This indicates that the model cannot provide an adequate representation of the data. Also, the fitted Gaussian width is much greater than the instrumental resolution, suggesting that the data contain an additional contribution to the spectrum. This is in line with earlier work,[1] in which the authors suggested that there is possibly a third spin-orbit doublet whose properties, however, they could not reliably determine. Thus in Fig. 2(b) we reanalyze the data with a three-doublet model. The decreased magnitude of the residuals and the absence of oscillations mark this as a satisfactory model; furthermore, the Gaussian width is 0.3 eV, consistent with the analyzer-limited resolution of 0.25 eV plus some photon broadening.

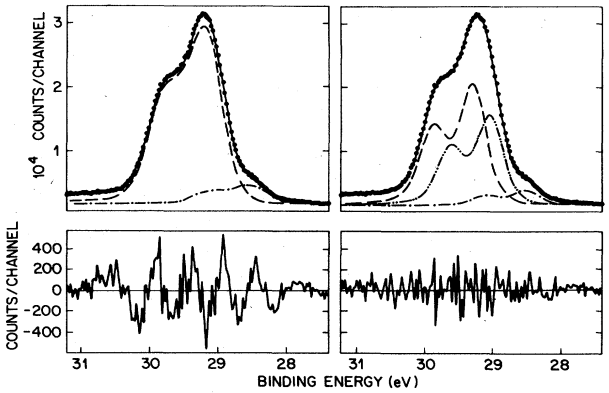

FIG. 2. Least-squares fits to the Ge $3d$ photoemission spectrum of a clean Ge(111) surface: (a) with two spin-orbit doublets, and (b) with three spin-orbit doublets. The differences between the data points and the fitted line, shown on a greatly expanded scale below each fit, make clear the preference for a three-doublet model.

A reasonable question at this point is whether the two

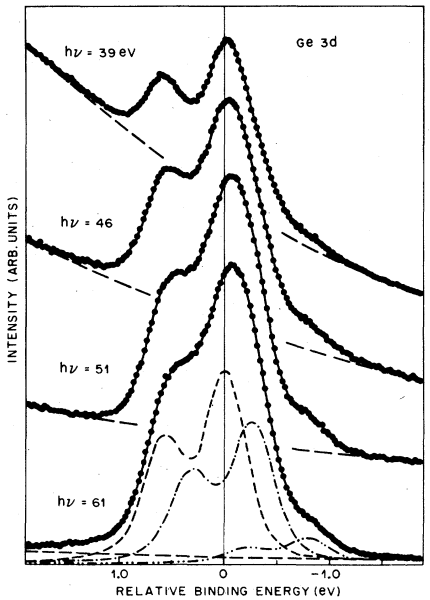

FIG. 3. Comparison of the photoemission spectra of clean Ge(111) taken at four different photon energies. The zero of the energy scale is placed at the Ge $3d_{5/2}$ binding energy of bulk germanium (29.6 eV). The solid lines through the data points are the results of least-squares fits with three spin-orbit doublets which are shown only for the highest photon energy.

closely spaced components that make up the main line are physically significant, or are merely a convenient way of representing the data. An answer is obtained from data taken over a range of photon energies and shown in Fig. 3.

At lower photon energy the escape depth increases markedly, and the fractional contribution from the surface atoms is reduced relative to that from the bulk atoms. At the lowest photon energy the kinetic energy of the photoelectrons is ~ 10 eV with respect to the Fermi level, $E_F = 0$ eV, making the escape depth large compared to the layer spacing of Ge(111). The dominance of the component at greatest binding energy identifies it as being due to photoelectrons from the bulk atoms. This component does, in fact, lie at the bulk binding energy, $E_B = 29.6$ eV. The two components at smaller binding energy then originate from surface atoms and contain information regarding the surface reconstruction.

The qualitative observations regarding the photon-energy dependence of these spectra are confirmed by detailed least-squares analysis. The results shown in Fig. 4(b) confirm that the binding energies of the two surface components are independent of photon energy. If this were not true, one would have to reject the data analysis as unreliable. More interesting is the quantitative result for the intensities in Fig. 4(a), which shows the attenuation of the two surface components as the kinetic energy decreases. The fractional intensities obtained from these fits can be used, together with the estimated escape depth[15] of 4.9 Å at 34 eV kinetic energy, to estimate the number of Ge atoms contributing to these surface components. Correcting for the experimental geometry, one finds that for the clean Ge(111) sample the total surface signal corresponds to 1.57 ML of Ge atoms. Below, we shall refer to the fractional intensity of the component D_2 at lowest binding energy as S_2, to the fractional intensity of the other surface component D_1 as S_1, and to that of the bulk as S_0.

The estimated number of atoms contributing to each surface component depends somewhat on what assumptions are made about the surface structure. For example, if S_2 represents surface atoms and S_1 represents *subsurface* atoms, then S_2 corresponds to 0.24 ML and S_1 to 1.33 ML of Ge atoms on the clean surface. If there is no distinguishable subsurface layer, then these values become 0.32 and 1.25 ML, respectively. These estimates have an overall multiplicative uncertainty associated with the uncertainty of the value used for the escape depth.

D. Tin coverage dependence of core-level spectra

Figures 5 and 6 show the evolution of the intensities and binding energies of the Ge $3d$ and Sn $4d$ spectra as the Sn coverage is increased. Given the dramatic changes that the LEED pattern undergoes as the Sn coverage increases from 0 to 0.3 ML, one might have expected substantial rearrangement and perhaps replacement of the Ge surface atoms by Sn atoms. Surprisingly, however, the

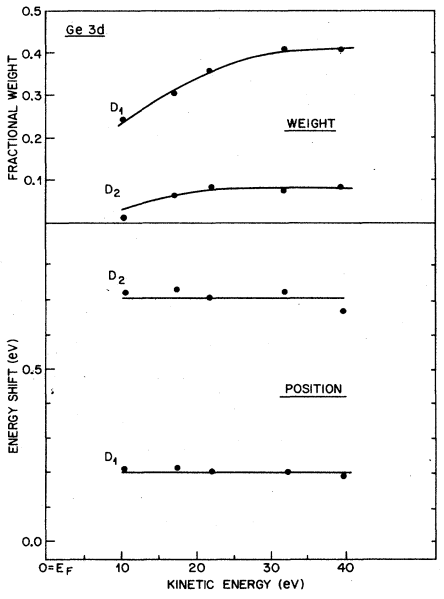

FIG. 4. Numerical results of the least-squares analysis shown in Fig. 3. D_1 and D_2 refer to the two components at smaller binding energy. Their identification as surface components is confirmed by the decrease in their weight with decreasing kinetic energy (increasing escape depth).

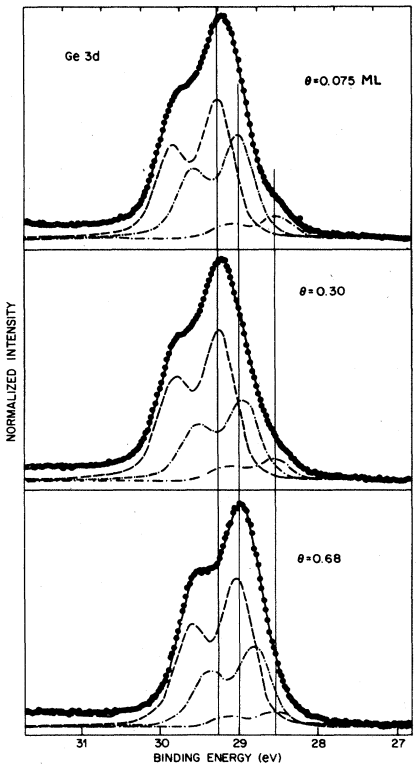

FIG. 5. Modification of the Ge $3d$ spectrum by submonolayer coverage with Sn. The solid lines through the data points are the results of least-squares fits made with three spin-orbit doublets, shown as dashed lines. The decrease in relative intensity of the larger surface component between 0.075 and 0.30 ML coverage coincides with the 2×2-to-7×7 transition.

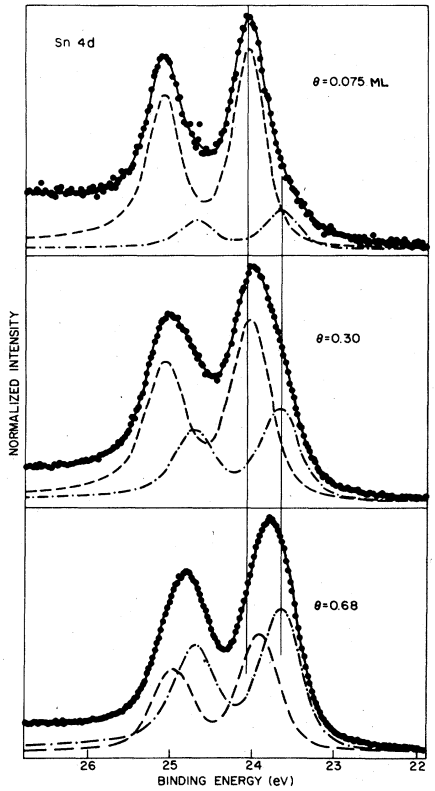

FIG. 6. Photoemission spectra of the Sn 4*d* electrons for submonolayers of Sn deposited on clean Ge(111). The solid lines through the data points are the results of least-squares fits made with two spin-orbit doublets, shown as dashed lines. Only the intensities, and not the energies, of the two doublets change between 0.075 and 0.30 ML coverage.

changes in the Ge and Sn photoemission spectra are relatively subtle. The Sn 4*d* spectra show two inequivalent tin atoms in the overlayer even at the smallest coverages studied (see Fig. 6). A satisfactory fit to the data was obtained with two spin-orbit doublets as shown in Fig. 6, with the relative intensities of the doublets varying with coverage. The component at greater binding energy dominates at low coverage and then saturates, while the one at smaller binding energy continues to grow.

IV. DISCUSSION

A. Core-level spectral intensities

The Ge 3*d* and Sn 4*d* integrated core-line intensities versus total Sn coverage for a photon energy of 61 eV, is shown in Fig. 7. The kinetic energies are ~28 and 33 eV for the germanium and tin photoelectrons. The Sn intensity grows linearly up to ~1 ML, at which point there is an abrupt decrease in the slope. This appears to rule out island growth of the tin and suggests instead that the first monolayer of tin fills in before further growth occurs. Both from the attenuation of the Ge signal and the Sn intensity at 1 ML coverage, we estimate an overlayer thick-

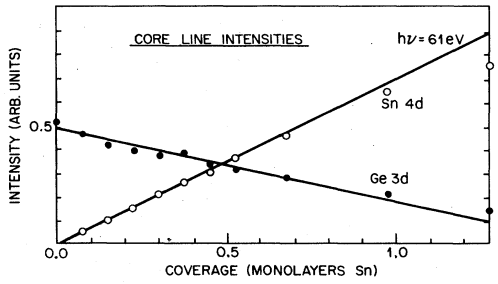

FIG. 7. Strengths of the Ge 3*d* and Sn 4*d* signals as a function of tin-overlayer thickness. The abrupt break at 1 ML from the linear increase of Sn intensity indicates layer-by-layer growth of the Sn.

ness of one photoelectron mean free path at 1.4—1.5 ML of Sn coverage; considering our experimental geometry, this implies an escape depth in tin of ~2 ML, or ~6 Å.

A separate run was made to investigate the effect of annealing on the coverage. This showed that below ~1 ML the coverages remained unchanged to within 5%. This behavior changed rather abruptly for coverages above 1 ML, where the tin coverage was substantially reduced by annealing. This is most likely due to the evaporation of tin from the surface and possibly to interdiffusion. The sample can be leached clean of tin by sputtering for ~10 min with the sample held at 550 °C.

B. Submonolayer Sn coverage dependence of Ge 3*d* spectra

Figures 8 and 9 show the relative intensities and binding energies for Ge and Sn, respectively, as a function of Sn coverage. During submonolayer deposition of Sn on Ge(111) the fractional intensity of the D_2 component of the Ge spectrum is nearly constant, while the fractional intensity of D_1 decreases. The simplest explanation of this observation is that the adsorbed Sn interacts with a

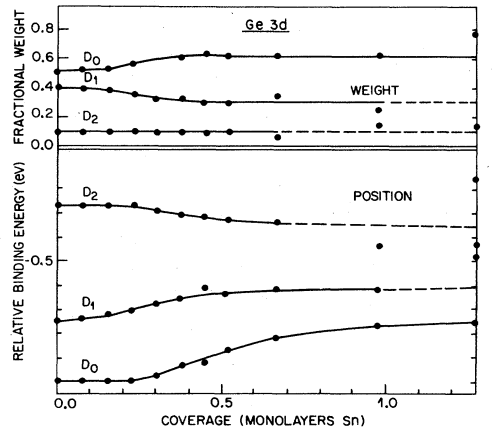

FIG. 8. Results of least-squares analyses of Ge 3*d* spectra with submonolayer Sn coverage. The intensity of the surface component D_2 is constant. The binding-energy shift of the bulk component D_0 is due to band bending at the surface.

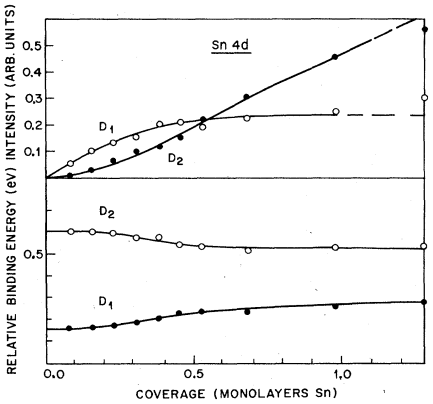

FIG. 9. Results of the least-squares analysis of Sn $4d$ spectra of submonolayer Sn on Ge(111). Note the saturation of the D_1 site and the continued growth of the D_2 site.

portion of the D_1 atoms and causes their core-electron binding energy to become similar to the bulk value, causing D_1 atoms to decrease as D_0 atoms increase. Apparently the adsorbed Sn and the reordering of the surface have no such effect on the atoms contributing to D_2. Beginning at ~ 0.2 ML, band bending manifests itself in the binding-energy shift of the bulk component.

The constant D_2 intensity implies that the local environment of that subset of surface atoms is undisturbed by the transition from $c(2\times 8)$ to 7×7 order. This is presumably also true for the atoms that continue to contribute to D_1 intensity at Sn coverages above 0.3 ML. This suggests that there are building blocks, smaller than either unit cell, that are the same in both reconstructions. We also observed that, at low coverages, annealing the sample caused the higher-binding-energy Sn $4d$ component to grow at the expense of the other. The straightforward inference is that the Ge(111) surface contains 0.25 ML of favorable adsorption sites that the Sn atoms occupy first, causing one Ge atom per site to become bulklike. It may be significant that as these favorable sites fill, or as Sn begins to adsorb in different sites, the 7×7 reconstruction occurs. At higher coverages (>0.5 ML), the two Sn components become difficult to separate by least-squares fitting.

C. Implications for surface reconstruction

Interest in the 7×7 reconstruction of the Si surface has resulted in extensive work on a variety of structural models. The close similarity of electron-diffraction results for the Sn-induced 7×7 reconstruction of the Ge(111) surface and the clean Si(111)7×7 structure suggests that these surfaces are nearly identical. Thus, Si(111)7×7 models provide a natural framework for interpretation of our photoemission data.

Before considering particular models, we summarize the implications of our data. First, to be consistent with our core-level spectra, a model of the Ge(111)2×8 and Ge(111)7×7 reconstructed surfaces must have at least two inequivalent surface Ge atoms with relative populations of approximately $1{:}4\pm 1$. Of course, the data are also consistent with the existence of more than two types of surface atoms. In addition, our data clearly imply that Sn does *not* replace Ge in a random fashion as suggested by Higashiyama and co-workers,[16] but instead seems to replace or to modify only atoms included in the larger group of Ge surface atoms identified as peak D_1. The total number of such atoms modified by Sn adsorption is 0.25—0.32 ML. It is possible that adsorbed Sn preferentially replaces the certain Ge atoms that are twofold coordinated. Such twofold coordination implies an s^2p^2 electronic configuration, which, in bulk compounds, is more stable for Sn than for Ge because of the larger s-p atomic splitting in the sequence C, Si, Ge, Sn, and Pb, relative to the s-p—hybridization energy gain in forming tetrahedral sp^3 bonds.

Our data also suggest that the Sn atoms do not penetrate deep into the bulk layers. If the 2×8 structure of the clean Ge(111) surface is a slight variation of the 2×1 reconstruction of cleaved Ge(111) and Si(111), then there will be 0.5 ML of "special" sites; that would be completely at variance with the core-level spectra from the clean Ge surface.

D. Comparison with structural models of Si(111)7×7 surface

In this section we discuss the compatibility of our Sn/Ge(111) photoemission core-level studies with several previously proposed structural models of Si(111)7×7. Attempts to interpret this reconstruction date back more than 25 years to the Schlier-Farnsworth-Haneman buckling models[17] and the Lander vacancy model.[18] We also consider some of the more recent island and adatom models proposed in response to diffraction and tunneling-microscope results.

1. Lander vacancy model

This model[18] assumes a 2×2 periodicity with a glide plane within the unit mesh. We discuss short-range surface-site effects (appropriate to our core-level results) in terms of the smaller 2×2 mesh. There are three surface atoms and three second-layer atoms with unsaturated bonds, as well as a surface-vacancy site within the 2×2 unit cell. The 1:3 ratio of vacancies to top-layer sites is close to the ratio of D_1-type Sn to D_1-type Ge atoms for the 7×7 Ge(111) surface. However, this model offers no explanation for the D_2-type Ge atoms, which occur on both the clean and the Sn-covered surfaces.

2. Haneman-Chadi buckling model

Buckling is generally not thought to occur for Si(111)7×7, but such a reconstruction could be stabilized by ring formation, as discussed by Chadi.[19] However, this type of reconstruction also involves a half-layer, that is, it has 2×1 local order, and cannot easily lead to the 4:1 ratio of D_1- to D_2-type Ge atoms unless there are different amounts of buckled displacements in this structure.

3. *Harrison-Lander adatom models*

This model was originally proposed by Lander[20] for Al, In, and P impurity-induced reconstructions, and was later modified by Harrison[21] for clean Si(111) and Ge(111) surfaces. It has gained popularity in the last year and a half by providing a basis for the interpretation of scanning-tunneling-microscope images[22] of the Si(111)7×7 unit mesh. In this model there are 0.25—0.33 ML of Ge adatoms for Ge(111)2×8 that should be replaced by Sn atoms, since the larger atomic radius of Sn allows less strain in the adatom—to—surface-atom bonds. However, the presence of ~0.25 ML of D_2-type Ge atoms which are *not* affected by the Sn leads to a conflict between our data and the simple adatom-type model.

4. *Aono-Snyder "tripedal" models*

The authors of Ref. 23 describe a model of the 7×7 Si(111) surface involving "milk stools" that consist of a pyramid of four atoms.[24] In this model the bulk terminates in an intact double layer above which lie the pyramids, each in registry with three of the substrate atoms in the upper single layer. In each 7×7 unit cell there are 12 pyramids, leaving 13 substrate atoms with dangling bonds. One can also construct a pyramid model that has the $c(2\times8)$ symmetry of clean Ge(111) surface. In this case each 16-atom cell contains four pyramids and four substrate atoms with dangling bonds, and has the periodicity proposed in Ref. 25. This periodicity produces all of the LEED features observed for the $c(2\times8)$ surface.

To relate this model to our photoemission data, we identify D_2, the component at lowest binding energy, with the top atoms of the pyramids. On the clean surface we observe approximately 4 times as many D_1-type Ge atoms as D_2-type atoms, and hence we assign to D_1 both the other three atoms in each pyramid and the substrate atoms with dangling bonds. For the Sn-induced 7×7 reconstruction, we reassign the atoms that had dangling bonds to the bulk component of the spectrum. This reassignment is reasonable if the Sn atoms have adsorbed at the dangling-bond sites on the Ge substrate, causing these Ge atoms to become bulklike.

5. *McRae-Cardillo island model*

The model of the 7×7 Si(111) surface proposed by McRae in Ref. 26 invokes stacking faults and dimerization and is a refinement of the earlier island models of McRae and Cardillo.[27] For this model, the distinguishable surface atoms are those involved in the dimers, of which there are 0.37 ML, and the remaining atoms in the surface layer, of which there are 0.61 ML. In the subsurface layer there are again 0.37 ML involved in dimers. These numbers cannot be reconciled with the measured magnitudes of the surface components for reconstructed Ge(111). Hence this model, regardless of its appropriateness for Si(111), does not seem to describe the Sn-induced reconstruction of Ge(111).

V. SUMMARY AND CONCLUSIONS

Core-level photoemission with synchrotron radiation has been used to study the various surface reconstructions, 2×8, 2×2, 7×7, and 5×5, that occur as a function of Sn coverage on Ge(111) surfaces. We find three separate Ge core-level components and two separate Sn components, suggesting at least one bulk and two inequivalent surface atoms for Ge and two inequivalent surface Sn atoms. From solid-solubility considerations and from our own photoemission intensities versus coverage and annealing, we rule out significant alloying.

There is an apparent selective modification of one type of surface Ge by Sn, but surprisingly it is the surface component D_1 with greater binding energy and a larger number of atoms rather than the weaker, lower-binding-energy D_2-type Ge atoms that are modified. This behavior is somewhat suggestive of the possibility that the D_1 component is actually two unresolved components. In comparing these results to five different classes of models for the surface-reconstruction mechanism, we find that some type of modified adatom unit, such as the "tripedal" four-atom cluster discussed by Aono *et al.* and by Snyder, fits the data best. Unfortunately, the somewhat limited resolution of our data, 200—250 meV, does not allow us to make a more conclusive identification of the surface mechanism. However, we have found new, quantitative experimental bounds that any proposed model of these surfaces must satisfy.

---

*Present address: Arizona State University, Tempe, AZ 85281.
†Present address: University of California, Berkeley, CA 94720.
‡Present address: Laboratoire pour l'Utilisation du Rayonnement Electromagnétique, Orsay Cedex, France.
§Present address: University of Florida, Gainesville, FL 32611.

[1]F. J. Himpsel, D. E. Eastman, P. Heimann, B. Reihl, C. W. White, and D. M. Zehner, Phys. Rev. B **24**, 1120 (1981).
[2]F. J. Himpsel, Physica (Utrecht) **117A&B**, 767 (1983).
[3]D. J. Chadi, J. Phys. Soc. Jpn. Suppl. A **49**, 1035 (1980).
[4]G. V. Hansson, R. Z. Bachrach, R. S. Bauer, and P. Chiaradia, J. Phys. Soc. Jpn. Suppl. A **49**, 1043 (1980); Phys. Rev. Lett. **46**, 1033 (1981).
[5]J. C. Phillips, Phys. Rev. Lett. **45**, 905 (1980).
[6]S. Brennan, J. Stöhr, R. Jaeger, and J. E. Rowe, Phys. Rev. Lett. **45**, 1414 (1980).
[7]D. E. Eastman, T.-C. Chiang, P. Heimann, and F. J. Himpsel, Phys. Rev. Lett. **45**, 656 (1980).
[8]C. D. Thurmond and M. Kowalchik, Bell Syst. Tech. J. **39**, 169 (1960).
[9]T. Ichikawa and S. Ino, Surf. Sci. **105**, 395 (1981).
[10]We acknowledge the help of L. C. Feldman in these measurements. More detailed studies by channeling of the lattice location of Sn/Ge(111) are in progress.
[11]J. E. Rowe, H. Froitzheim, and H. Ibach, Surf. Sci. **48**, 44 (1974).
[12]T. Ichikawa and S. Ino, Solid State Commun. **34**, 349 (1980).
[13]D. W. Marquardt, J. Soc. Indust. Appl. Math. **11**, 431 (1963).
[14]S. Doniach and M. Šunjić, J. Phys. C **3**, 285 (1970).
[15]T. Miller, E. Rosenwinkel, and T. C. Chiang, Solid State Commun. **47**, 935 (1983).

[16]K. Higashiyama, S. Kono, H. Sakurai, and T. Sagawa, J. Phys. Soc. Jpn. (to be published).
[17]D. Haneman, Phys. Rev. **121**, 1093 (1961), and references therein.
[18]J. J. Lander and J. Morrison, J. Appl. Phys. **34**, 1403 (1963).
[19]D. J. Chadi, Phys. Rev. Lett. **41**, 1062 (1978); Phys. Rev. B **19**, 2074 (1979).
[20]J. J. Lander and J. Morrison, J. Appl. Phys. **36**, 1706 (1965).
[21]W. A. Harrison, Surf. Sci. **55**, 1 (1976).
[22]G. Binnig, H. Rohrer, Ch. Gerber, and E. Weibel, Phys. Rev. Lett. **50**, 120 (1983).
[23]M. Aono, R. Souda, C. Oshima, and Y. Ishizawa, Phys. Rev. Lett. **51**, 801 (1983).
[24]L. C. Snyder, Z. Wasserman, and J. W. Moskowitz, J. Vac. Sci. Technol. **16**, 1266 (1979); L. C. Snyder (unpublished).
[25]P. W. Palmberg and W. T. Peria, Surf. Sci. **6**, 57 (1967).
[26]E. G. McRae, Phys. Rev. B **28**, 2305 (1983), and references therein.
[27]M. J. Cardillo, Phys. Rev. B **23**, 4279 (1981).